Structure of Supercooled Aqueous Zinc(II) Bromide Solutions by Raman and X-Ray Scattering Methods

Toshiyuki Takamuku*, Kazumasa Yoshikai, Toshio Yamaguchi, and Hisanobu Wakita

Department of Chemistry, Faculty of Science, Fukuoka University, Nanakuma, Jonan-ku, Fukuoka 814-01, Japan

Z. Naturforsch. **47a**, 841–848 (1992); received April 24, 1992

The structure of aqueous zinc(II) bromide solutions with $[H_2O]/[ZnBr_2]$ molar ratios 5 and 10 in the supercooled state and at ambient temperature has been investigated by Raman spectroscopy and X-ray scattering. Raman spectra of glassy solutions have also been measured for comparison. The Raman and X-ray data suggest that tetrabromo and hexaaqua zinc(II) complexes are favoured in the supercooled and glassy state, while dibromo- and tribromozinc(II) complexes are formed as main species in the solutions at ambient temperature. Probably the reactions

$$2\,[ZnBr_2(OH_2)] + 2\,H_2O \rightarrow [ZnBr_4]^{2-} + [Zn(OH_2)_6]^{2+}$$

and

$$4\,[ZnBr_3(OH_2)]^- + 2\,H_2O \rightarrow 3\,[ZnBr_4]^{2-} + [Zn(OH_2)_6]^{2+}$$

occur in the supercooled and glassy solutions. These equilibrium shifts are discussed.

Key words: Supercooled solution, Zinc(II) bromide, Raman spectroscopy, X-ray diffraction, Structure.

1. Introduction

Zinc(II) halides, which are very hygroscopic and highly soluble in water, form supercooled and glassy solutions, the structure of which has recently been studied [1–4].

Structural investigations of aqueous zinc(II) halide solutions, at ambient temperature, using X-ray diffraction and Raman spectroscopy [5–13], have suggested that tetrahedral complexes, $[ZnX_n(OH_2)_{4-n}]^{(2-n)+}$ (X^- = halide ion), are formed. X-ray diffraction studies on concentrated aqueous zinc(II) halide solutions have shown that the complexes $[ZnX_2(OH_2)_2]$ and $[ZnX_3(OH_2)]^-$ are predominantly formed at ambient temperature [5, 7, 8].

Yang et al. [14] have measured Raman spectra of aqueous zinc(II) bromide solutions at high temperature up to 300 °C and pressures up to 9 MPa. Our X-ray diffraction studies on concentrated aqueous zinc(II) bromide solutions at temperatures up to 140 °C [15] have suggested that the lower complex, $[ZnBr_2(OH_2)_2]$, gets more favoured than the highest complex, $[ZnBr_4]^{2-}$, at higher temperatures.

Raman spectra of glassy aqueous zinc(II) halide solutions ($[H_2O]/[ZnX_2] = 10$, $X = Cl^-$, Br^-, and I^-), prepared by quick vitrification in liquid nitrogen, have been taken by Kanno and Hiraishi [1]. They concluded that the complexes $[ZnX_4]^{2-}$ and $[Zn(OH_2)_6]^{2+}$, produced by the shift

$$2\,ZnX_2 + 6\,H_2O \rightarrow [ZnX_4]^{2-} + [Zn(OH_2)_6]^{2+}, \qquad (3)$$

are favoured in the glassy solution while $[ZnX_2(OH_2)_2]$ is unstable.

X-ray absorption fine structure (XAFS) measurements on glassy aqueous zinc(II) halide solutions have confirmed that $[ZnX_4]^{2-}$ and $[Zn(OH_2)_6]^{2+}$ are predominantly formed in the glassy solutions [3, 4]. A low equilibrium constant (ca. 0.04) for (3) at ambient temperature [16] supports the Raman and XAFS results.

Since the equilibrium (3) depends on the ion-ion, ion-water, and water-water interactions, the investigation of the microscopic structure of the supercooled solutions is essential to interpret the thermodynamic and Raman data and to understand the vitrification and crystallization processes of aqueous electrolyte solutions. To our knowledge, there are few reports on structural studies of supercooled aqueous zinc(II)

* On leave from Aqua Laboratory, Research and Development Division, TOTO Ltd., Nakashima, Kokurakita-ku, Kitakyushu 802, Japan.

Reprint requests to Prof. T. Yamaguchi, Department of Chemistry, Faculty of Science, Fukuoka University, Nanakuma, Jonan-ku, Fukuoka 814-01, Japan.

0932-0784 / 92 / 0700-0841 $ 01.30/0. – Please order a reprint rather than making your own copy.

halide solutions except our previous investigation of supercooled aqueous zinc(II) iodide solutions [2].

In the present study we have examined supercooled aqueous zinc(II) bromide solutions. Raman spectral measurements are performed from ambient to liquid nitrogen temperatures. Moreover, X-ray diffraction measurements are made to determine the average structure of the chemical species at ambient and supercooled temperatures. Raman spectra of the glassy solutions are also measured to confirm the previous results [1]. Finally, we discuss the equilibrium shift with temperature and its anion effect from a structural point of view with respect to the ion-ion, ion-water, and water-water interactions.

2. Experimental

2.1. Preparation of Sample Solutions

Zinc(II) bromide (Wako Pure Chemicals, 99.9%), without purification, was dissolved in distilled water to reach the $[H_2O]/[ZnBr_2]$ molar ratios 5 and 10. Concentrations of zinc(II) in the sample solutions were determined by titration with an EDTA standard solution using Eriochrom Black T (EBT) as an indicator. The densities of the solutions at 25 °C were measured pycnometrically, but those of the corresponding supercooled solutions were estimated from extrapolation of the densities measured at temperatures from 5 to 100 °C [17]. Properties of the sample solutions at 25 °C are given in Table 1.

The glass transition temperature of solution A was found to be − 97 °C by differential scanning calorimetry. Thus, all Raman and X-ray scattering measurements on the supercooled solutions were carried out above − 80 °C.

2.2. Raman Spectral Measurements

Each sample solution was sealed into a glass tube of 1.8 mm inner diameter. Raman spectra for sample solutions A and B were recorded at 25, − 5, − 20, − 40, − 60, and − 80 °C on a JEOL JRS-400 T spectrometer using the 514.5 nm line radiated from an argon ion laser (Spectra Physics Model 168 B). The temperature of the supercooled solutions was controlled by blowing cooled dry nitrogen gas on the samples. Raman spectra for the glassy samples were measured by immersing the sample tubes into liquid nitrogen (− 196 °C).

Table 1. Concentrations (mol/kg H_2O), densities ϱ (g cm^{-3}) at 25 °C, the stoichiometric volumes V (10^8 pm^3) per Zn atom and water/salt molar ratios.

	Solution A	Solution B
Zn^{2+}	10.64	5.493
Br^-	21.28	10.99
ϱ	2.198	1.761
V	2.412	3.841
$[H_2O]/[ZnBr_2]$	5.217	10.11

2.3. X-ray Diffraction Measurements

X-ray diffraction measurements for solution A were carried out with a Rigaku $\theta - \theta$-type diffractometer using Mo $K\alpha$ radiation ($\lambda = 71.07$ pm). Scattered X-rays were monochromatized by an LiF (200) crystal. The scattering angles (2θ) ranged from 2° to 140°, corresponding to scattering vectors s ($= 4\pi \sin\theta/\lambda$) of 3.1×10^{-4} to 0.166 pm^{-1}. Different slit combinations and step angles were used depending on the angle range. The measurements were repeated twice over the whole angle range; the total amounts of X-rays collected at each angle were 80 000 at 25 and − 5 °C and 40 000 counts at − 20 and − 40 °C. Details of the X-ray measurements have been described elsewhere [18, 19]. The temperature of the sample solutions was measured with a copper-constantan thermocouple and was controlled within ± 0.2 °C by using a cryostat system described in [2].

2.4. X-ray Data Treatment

The measured intensities were corrected for background, absorption, polarization, multiple scatterings, and incoherent scattering of X-rays in the usual way [20]. The reduced intensities $i(s)$ are given as

$$i(s) = K I(s) - \sum_i x_i f_i^2(s), \tag{4}$$

where K is a normalization factor of the observed intensities $I(s)$ to the absolute unit, x_i is the number of atoms i in the stoichiometric volume V containing one Zn atom, and $f_i(s)$ is the atomic scattering factor of atom i corrected for anomalous dispersion. The $si(s)$ values are Fourier transformed into the radial distribution function $D(r)$ as

$$D(r) = 4\pi r^2 \varrho_0 + \frac{2r}{\pi} \int_0^{s_{max}} s\, i(s)\, M(s) \sin(r s)\, ds. \tag{5}$$

Here, ϱ_0 ($= [\sum x_i f_i(0)]^2/V$) is the average electron density in the stoichiometric volume V, s_{max} is the

maximum s-value attained in the measurements ($s_{max} = 0.166\ pm^{-1}$). A modification function $M(s)$ of the form $[\sum x_i f_i^2(0)/\sum x_i f_i^2(s)] \exp(-100 s^2)$ was used for the sample solutions.

The theoretical intensities $i(s)_{calc}$ were calculated on the basis of a model

$$i(s)_{calc} = \sum_{\substack{ij \\ i \neq j}} \sum x_i n_{ij} f_i(s) f_j(s) \frac{\sin(r_{ij} s)}{r_{ij} s} \exp(-b_{ij} s^2) - \sum_{\substack{ij \\ i \neq j}} \sum x_i x_j f_i(s) f_j(s) \frac{4\pi R_j^3}{V} \frac{\sin(R_j s) - R_j s \cos(R_j s)}{(R_j s)^3} \exp(-B_j s^2). \quad (6)$$

The first term on the right-hand-side of (6) is related to short-range interactions characterized by the interatomic distances, r_{ij}, the temperature factor, b_{ij}, and the number of interactions, n_{ij}, for atom pair $i - j$. The second term arises from the interaction between a spherical hole and the continuum electron distribution beyond the discrete distance. R_j is the radius of the spherical hole around atom j and B_j is the softness parameter for emergence of the continuum electron distribution.

A comparison between the experimental and the theoretical structure functions was made with a least-squares refinement procedure of minimizing the error square sum,

$$U = \sum_{s_{min}}^{s_{max}} s^2 \{i(s)_{exp} - i(s)_{calc}\}^2. \quad (7)$$

All calculations of the X-ray diffraction data were performed with programs KURVLR [20] and NLPLSQ [21].

3. Results

3.1. Raman Spectra

Raman spectra for solutions A and B at various temperatures are shown in Figure 1. Three intense Raman bands are observed at 207, 185, and 172 cm^{-1} at 25 °C for both solutions; the peaks are assigned to the ν_1 mode of the totally symmetric Zn–Br vibration within the dibromo-, the tribromo-, and tetrabromozinc(II) complexes, respectively, according to previous investigations by Kanno and Hiraishi [1]. Yang et al. [14] have reported that a Raman band for the monobromozinc(II) complex appears at 240 cm^{-1} for a 3.72 m aqueous zinc(II) bromide solution at 200 °C. As seen in Fig. 1 for the present solutions, the band for the monobromo species is not observed; thus the monobromozinc(II) complex is not formed in solutions A and B, or, if any, the formation is too small to be detected. Kanno and Hiraishi [1] have reported that the intensity of the ν_1 band for the tetrabromozinc(II) complex increases while that for the dibromo- and the tribromozinc(II) complexes decreases when an aqueous solution of $ZnBr_2 \cdot 10H_2O$ is quenched from room temperature to the glassy state at liquid nitrogen temperature. As seen in Fig. 1, the spectral intensity starts to change even at − 5 °C. Thus it is concluded that the equilibrium shift (3) does occur in the supercooled solution and hence is not caused by the vitrification process. With lowering temperature the intensity of the ν_1 band for the tetrabromo species increases gradually, while that for the dibromo species decreases. Interestingly, the intensity of the ν_1 band for the tribromozinc(II) complex also decreases with decreasing temperature. This finding is in marked contrast with the result obtained for the aqueous zinc(II) iodide solution where the ν_1 band for the triiodozinc(II) complex does not change significantly with temperature [2]. As seen in Fig. 1, the change of intensity for the three Raman bands at 207, 185, and 172 cm^{-1} is more drastic for the water-rich solution B than for solution A.

A broad Raman band around 390 cm^{-1} of solution B at various temperatures is shown in Figure 2. The band is assigned to the ν_1 mode of the totally symmetric Zn–O vibration within the aqua zinc(II) ion according to a Raman spectroscopic study of a 3.36 m aqueous zinc(II) nitrate solution by Bulmer et al. [22]. The intensity of the ν_1 band for the aqua zinc(II) ion increases with decreasing temperature; thus the aqua zinc(II) ion is more favoured in the supercooled solutions than at room temperature. With lowering temperature the peak position of the band apparently shifts to higher wavenumbers, indicating a change of the contribution of the hot band excitation with temperature [2, 22]. The broad contour over 390–500 cm^{-1} for the glassy state has been ascribed to the libration mode of water [2, 23, 24].

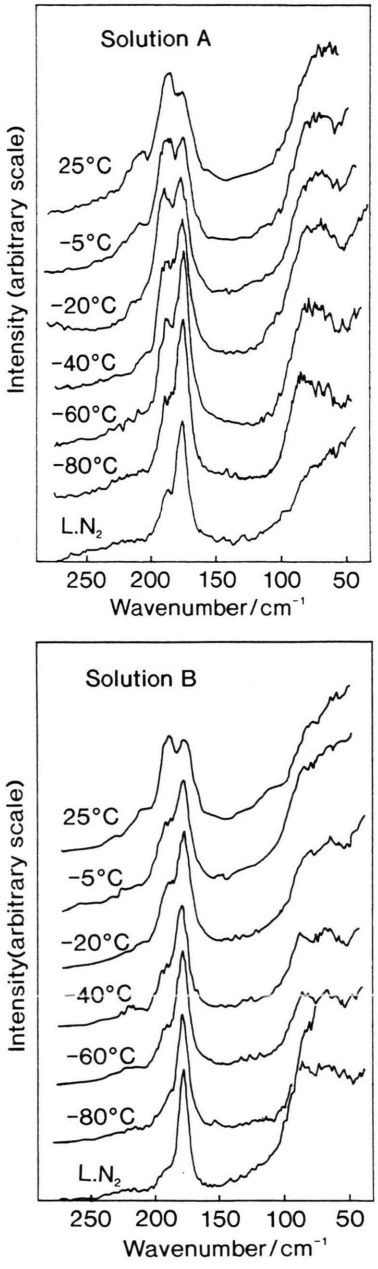

Fig. 1. Raman spectra for concentrated aqueous zinc(II) bromide solutions A and B at various temperatures. The spectrum at liquid nitrogen temperature corresponds to the glassy solution.

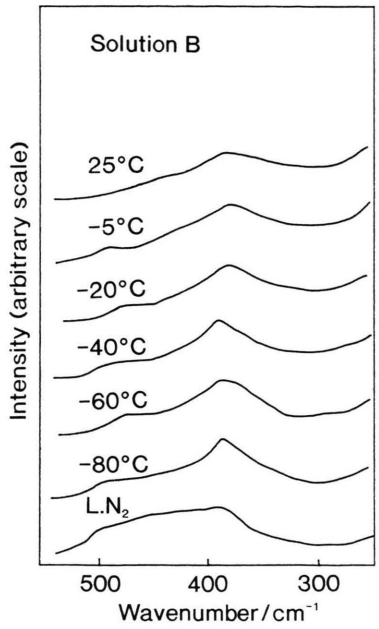

Fig. 2. Raman spectra of the concentrated aqueous zinc(II) bromide solution B at various temperatures. The spectrum at liquid nitrogen temperature corresponds to the glassy solution.

3.2. X-ray Scattering

The s weighted structure functions and the total radial distribution functions (RDFs), $D(r) - 4\pi r^2 \varrho_0$, for solution A at various supercooling temperatures are shown in Figs. 3 and 4, respectively. The total RDF arises mainly from interactions related to the bromide and zinc ions in the sample solution. In the RDFs at all temperatures two sharp and one broad peak appear at 239, 390, and 550–850 pm, respectively. The broad peak at 550–850 pm should be assigned to long-range interactions in the sample solution, which are too complex to be uniquely determined. The first peak originates mainly from the Zn–Br interactions within the zinc(II) bromo complexes present in the solution. A peak due to the Zn–O interactions within the aqua zinc(II) ion is expected to appear at about 210 pm [5–8], which is, however, hidden by the large peak of the Zn–Br interactions at 239 pm. The second peak is due mainly to nonbonding Br ··· Br interactions within the tetrahedral zinc(II) bromo complexes, because the ratio (1.63) of the Br ··· Br distance to the Zn–Br one is equal to an expected value ($[8/3]^{1/2} = 1.63$) for a tetrahedral coordination. The nonbonding Br ··· O(H_2O) interactions within the dibromo- and the tribromozinc(II) complexes, $[ZnBr_2(OH_2)_2]$ and $[ZnBr_3(OH_2)]^-$, also contribute to the peak at about 360 pm. In addition, the interactions between the ligating atoms within the zinc(II) complexes and water molecules in the second shell also appear to fall within 335–490 pm on the basis of

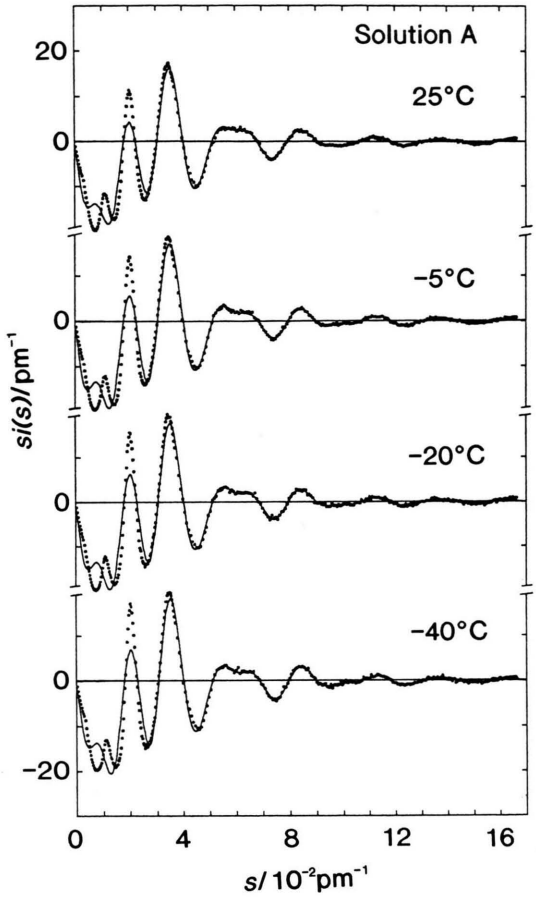

Fig. 3. Structure functions $i(s)$ multiplied by s for concentrated aqueous zinc(II) bromide solution A at various temperatures. The experimental values are drawn by dots and those calculated with the parameter values given in Tables 2 and 3 by solid lines.

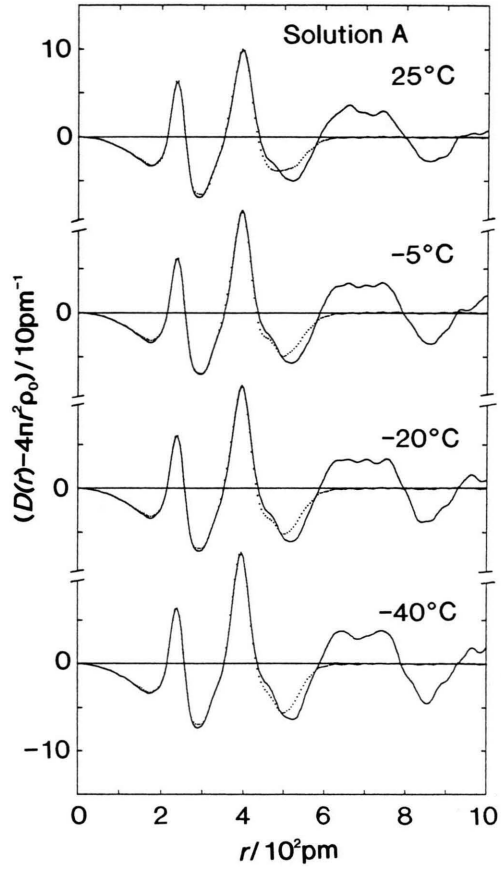

Fig. 4. Radial distribution functions $D(r) - 4\pi r^2 \varrho_0$ for concentrated zinc(II) bromide solution A at various temperatures: experimental (solid lines) and calculated (dots).

Table 2. Optimized parameter values of the interactions within the zinc(II) bromide complexes for solution A at various temperatures. Interatomic distance (r/pm), temperature factor (b/pm^2), and number of interactions (n) per zinc(II) ion. The values in parentheses are standard deviations of the last figure. The parameters without standard deviations were not allowed to vary in the calculations. [a] [3].

Interaction	Parameter	25 °C	− 5 °C	− 20 °C	− 40 °C	Glass[a] (Liquid N_2)
Zn–O	r	210	210	210	210	–
	b/10	5	5	5	5	–
	n	2.5	3.0	3.0	3.0	–
Zn–Br	r	238.2(1)	239.0(1)	239.0(2)	239.4(2)	238
	b/10	2	2	2	2	–
	n	1.97(2)	1.96(2)	1.96(2)	2.03(2)	2
Br ··· Br	r	391.3(4)	390.4(3)	391.1(4)	390.3(4)	–
	b/10	20	20	20	20	–
	n	1.88(4)	2.30(4)	2.38(6)	2.41(5)	–
Br ··· O	r	360	360	360	360	–
	b/10	10	10	10	10	–
	n	2.0	1.0	1.0	0.7	–

Table 3. Optimized parameter values of the medium range interactions and of the continuum electron distribution for solution A at various temperatures. Interatomic distance (r/pm), temperature factor (b/pm^2), number of interactions (n) per zinc(II) ion, and parameters for continuum electron distribution (R/pm and B/pm^2). The values in parentheses are standard deviations of the last figure. The parameters without standard deviations were not allowed to vary in the calculations.

Interaction	Parameter	25 °C	− 5 °C	−20 °C	− 40 °C
Zn ··· H_2O	r	401	399	399	396
	b/10	10	10	10	10
	n	10.5	10.6	10.2	11.8
Br–H_2O	r	335	337	337	333
	b/10	15	10	15	10
	n	4.3	4.0	4.9	5.0
Zn ··· H_2O	r	489	490	477	494
	b/10	10	10	10	10
	n	3.0	1.0	1.0	0.6
Br ··· H_2O	r	450	459	459	458
	b/10	10	10	20	20
	n	3.4	4.8	5.5	7.0
Zn	R	239(6)	248(7)	254(7)	258(7)
	B/10	10	10	10	10
Br	R	506(2)	508(2)	511(2)	515(2)
	B/10	96(13)	102(14)	86(13)	65(12)
H_2O	R	341(3)	336(3)	342(3)	355(3)
	B/10	10	10	10	10

the crystal structure of $KZnBr_3 \cdot 2H_2O$ [25]. As seen in Fig. 4, when the sample solution is cooled down, the second peak increases in intensity and gradually becomes shaper, whereas the first peak does not change significantly.

A quantitative analysis was performed to characterize structural parameters from the X-ray diffraction data with a least-squares method, which was applied to the structure functions over the scattering vector of $0.1 \times 10^{-2} < s/\text{pm}^{-1} < 0.166$. The interatomic distance r, the temperature factor b, the number of interactions n, and the parameters R and B for a continuum electron distribution were treated as variables in the fitting procedure. The optimized parameter values within the first coordination shell are summarized in Table 2, together with those in the glassy state determined from the XAFS analysis [3]. The structural parameters of some significant interactions between the zinc(II) complexes and water molecules in the second coordination shell and those for a continuum electron distribution are also listed in Table 3. As seen in Figs. 3 and 4, the theoretical $si(s)$ and RDF calculated by using the optimized parameter values in Tables 2 and 3 reproduce well the observed ones except the long-range interactions not taken into account in the present analysis.

The distances of Zn–Br and Br ··· Br interactions at 25 °C are 238.2(1) and 391.3(4) pm, respectively, which are in good agreement with the values reported in an X-ray investigation of aqueous zinc(II) bromide solutions at ambient temperature [7]. The number of Zn–Br interactions (n_{Zn-Br}), i.e. the average coordination number of bromide ions for one zinc(II) ion, shows little dependence on temperature and is about 2.0 in the three states. On the other hand, the number of nonbonding Br ··· Br interactions increases from 1.88(4) at 25 °C to 2.41(5) at − 40 °C. The difference in $n_{Br \cdots Br}$ at both temperatures is 0.53, which is beyond the estimated uncertainties in the present X-ray analysis. The present X-ray results thus show that a higher zinc(II) bromo complex such as the tetrabromozinc(II) complex is more often formed in the supercooled solution than at the ambient temperature. In addition, the aqua zinc(II) ion, the lowest species in the series of the zinc(II) bromo complexes, should also appear more often in the supercooled state because of no appreciable change in the average coordination number n_{Zn-Br} with temperature. These findings from the X-ray experiment are consistent with those from the Raman spectra described in the previous section.

4. Discussion

The present Raman and X-ray scattering data have revealed that in the supercooled and glassy aqueous zinc(II) bromide solutions the formation of the tetrabromozinc(II) complex, $[ZnBr_4]^{2-}$, and the aqua zinc(II) complex, $[Zn(OH_2)_6]^{2+}$, are favoured, while the dibromozinc(II) complex, $[ZnBr_2(OH_2)_2]$, is un-

stable, similar to the case of aqueous zinc(II) iodide solutions [2]. Moreover, the formation of the tribromozinc(II) complex, $[ZnBr_3(OH_2)]^-$, is less favoured in the supercooled and glassy states than at ambient temperature, in contrast with the stable triiodo species, $[ZnI_3(OH_2)]^-$, in the corresponding states. Therefore it is likely that both equilibrium shifts (1) and (2) take place in the aqueous zinc(II) bromide solutions with lowering temperature. The spectral change of the Raman bands (Fig. 1) has shown that the formation of the tetrabromozinc(II) complex is more promoted in solution B than in solution A. Thus, the higher the water content in the solution, the more are the equilibrium shifts (1) and (2) favoured.

We now discuss the equilibrium shifts (1) and (2) with temperature as revealed in the present and previous [2] studies on the supercooled aqueous zinc(II) bromide and iodide solutions. Kanno and Hiraishi [24] have measured Raman spectra for glassy aqueous $LiCl \cdot 8H_2O$ and $LiCl \cdot 10H_2O$ solutions. From the change in intensity of the OH stretching band of the water molecule they have stated that the basic water structure, disrupted by the dissolved ions at ambient temperature, is recovered partially in the glassy $LiCl \cdot 5H_2O$ and $LiCl \cdot 5D_2O$ solutions, respectively, have revealed that the hydrogen-bonded network of water molecules is enhanced up to the third nearest neighbors. With decreasing temperature, in particular below the melting point of water, thus, the water-water and ion-water interactions are greatly enhanced. The ion-ion interaction would not be altered appreciably with temperature, however. Thus, in the supercooled and glassy aqueous zinc(II) bromide solutions, water molecules dispelled from the first coordination shell of the tribromo species will be stabilized in reinforced hydrogen-bond networks and hence a bromide ion will more easily bind to the zinc(II) ion to form the tetrahedral complex than in the liquid at room temperature.

Next, the anion effect on the equilibrium shifts (1) and (2) is discussed. The stepwise enthalpies reported at 25 °C are ΔH_1° and $\Delta H_2^\circ = 0$, $\Delta H_3^\circ = 26.4$, $\Delta H_4^\circ = -28.4$ kcal mol^{-1} for the bromide complexes and $\Delta H_1^\circ = 0$, $\Delta H_2^\circ = 2.9$, $\Delta H_3^\circ = 10.3$, $\Delta H_4^\circ = -31.5$ kcal mol^{-1} for the iodide complexes [27]. The enthalpy of the tribromo complex is about twice as large as that of the triiodo complex, suggesting that the former species is less stable than the latter in the solutions. This different behaviour in the complex formation will be ascribed to the size of the anions. In the formation of the tetrahalogeno species, a bromide ion will bind more strongly to a zinc(II) ion than an iodide ion because of the higher electron density of the smaller bromide ion and less steric hindrance between the ligands. With lowering temperature, this tendency toward the tetrabromozinc(II) complex will increase since a water molecule dispelled from the first coordination shell of the tribromo species is stabilized in the strengthened hydrogen bonded net. In the aqueous zinc(II) iodide solutions, on the other hand, the fourth step may take place to a similar extent as the third step with decreasing temperature; consequently the amount of the triiodo species will not change greatly with temperature.

When the tetrabromozinc(II) complex increases in the supercooled and glassy aqueous zinc(II) bromide solutions, the aqua zinc(II) ion will be formed in a water-rich region to satisfy the stoichiometry of the solute in the solutions, as suggested from the present Raman spectra.

Finally, we comment the temperature dependence of the anion-water interaction. This interaction is electrostatically stronger for the small bromide ion than for the larger iodide ion. However, since in the present solutions there is not enough water to build up discrete hydration shells of the individual halide ions, it is unlikely that the water-halide ion interaction contributes significantly to the shifts (1) and (2). Therefore, the difference in the shifts (1) and (2) with temperature arises mainly from the affinity of the halide ions to the zinc(II) ion.

Acknowledgements

The authors thank Prof. Tohru Inoue for the use of a differential scanning calorimeter. All calculations were performed at the Computer Center of Fukuoka University. The present work was partially supported by a Grant-in-Aid for Scientific Research on Priority Area of "Molecular Approaches to Non-equilibrium Processes in Solutions" (No. 03231105) from the Ministry of Education, Science and Culture, Japan.

[1] H. Kanno and J. Hiraishi, J. Raman Spectrosc. **9,** 85 (1980).
[2] T. Takamuku, T. Yamaguchi, and H. Wakita, J. Phys. Chem. **95,** 10098 (1991).
[3] T. Yamaguchi, O. Yata, H. Wakita, and M. Nomura, Photon Factory Activity Report, National Laboratory for High Energy Physics, KEK-PF, Oho, Tsukuba, Japan **5,** 230 (1986).
[4] (a) T. Yamaguchi, K. Kamihata, H. Wakita, and M. Nomura, Photon Factory Activity Report, National Laboratory for High Energy Physics, KEK-PF, Oho, Tsukuba, Japan **6,** 45 (1988).
(b) T. Yamaguchi, Pure Appl. Chem. **62,** 2251 (1990).
[5] (a) D. L. Wertz and J. R. Bell, J. Inorg. Nucl. Chem. **35,** 137. (1973). (b) ibid. **35,** 861 (1973).
[6] T. Yamaguchi, S. Hayashi, and H. Ohtaki, J. Phys. Chem. **93,** 2620 (1989).
[7] P. L. Goggin, G. Johansson, M. Maeda, and H. Wakita, Acta Chem. Scand. **A 38,** 625 (1984).
[8] H. Wakita, G. Johansson, M. Sandström, P. L. Goggin, and H Ohtaki, J. Solution Chem. **20,** 643 (1991).
[9] D. E. Irish, Ionic Interactions, Vol. II (S. Petrucci ed.), Academic Press, New York 1971, pp. 239–246.
[10] (a) M. L. Delwaulle, C. R. Acad. Sci. **240,** 2132 (1955).
(b) M. L. Delwaulle, Bull. Soc. Chim. Fr. **1955,** 1294.
[11] D. E. Irish, B. McCarroll, and T. F. Young, J. Chem. Phys. **39,** 3426 (1963).
[12] D. F. C. Morris, E. L. Short, and K. Slater, Electrochim. Acta **8,** 289 (1963).
[13] M. P. Fontana, G. Maisano, P. Migliardo, and F. Wanderlingh, J. Chem. Phys. **69,** 676 (1978).
[14] M. M. Yang, D. A. Crerar, and D. E. Irish, J. Solution Chem. **17,** 751 (1988).
[15] T. Takamuku, M. Ihara, T. Yamaguchi, and H. Wakita, Z. Naturforsch. **47a,** 485 (1992).
[16] B. Gilbert, Bull. Soc. Chim. Belges. **76,** 493 (1967).
[17] O. Söhnel and P. Novotný, Physical Sciences Data 22, Densities of Aqueous Solutions of Inorganic Substances, Elsevier, New York 1985.
[18] H. Wakita, M. Ichihashi, T. Mibuchi, and I. Masuda, Bull. Chem. Soc. Jpn. **55,** 817 (1982).
[19] T. Yamaguchi, G. Johansson, B. Holmgerg, M. Maeda, and H. Ohtaki, Acta Chem. Scand. **A 38,** 437 (1984).
[20] G. Johansson and M. Sandström, Chem. Scr. **4,** 195 (1973).
[21] T. Yamaguchi, Doctoral Thesis, Tokyo Institute of Technology, 1978.
[22] J. T. Bulmer, D. E. Irish, and L. Ödberg, Can. J. Chem. **53,** 3806 (1975).
[23] H. Kanno and J. Hiraishi, Chem. Phys. Lett. **72,** 541 (1980).
[24] H. Kanno and J. Hiraishi, J. Phys. Chem. **87,** 3664 (1983).
[25] Von R. Holinski and B. Brehler, Acta Crystallogr. **B 26,** 1915 (1970).
[26] T. Yamaguchi, M. Yamagami, T. Kurisaki, and T. Takamuku, and H. Wakita, submitted for publication.
[27] S. A. Shchukarev, L. S. Lilich, and V. A. Latysheva, Zh. Neorg. Khim. **1,** 225 (1956).